

# PCCP

Accepted Manuscript



This is an *Accepted Manuscript*, which has been through the Royal Society of Chemistry peer review process and has been accepted for publication.

*Accepted Manuscripts* are published online shortly after acceptance, before technical editing, formatting and proof reading. Using this free service, authors can make their results available to the community, in citable form, before we publish the edited article. We will replace this *Accepted Manuscript* with the edited and formatted *Advance Article* as soon as it is available.

You can find more information about *Accepted Manuscripts* in the [Information for Authors](#).

Please note that technical editing may introduce minor changes to the text and/or graphics, which may alter content. The journal's standard [Terms & Conditions](#) and the [Ethical guidelines](#) still apply. In no event shall the Royal Society of Chemistry be held responsible for any errors or omissions in this *Accepted Manuscript* or any consequences arising from the use of any information it contains.

## Hydrophobic effect on supported ionic liquid phase Pd nanoparticles hydrogenation catalysts

Cite this: DOI: 10.1039/x0xx00000x

Received 00th January 2012,  
Accepted 00th January 2012

DOI: 10.1039/x0xx00000x

www.rsc.org/

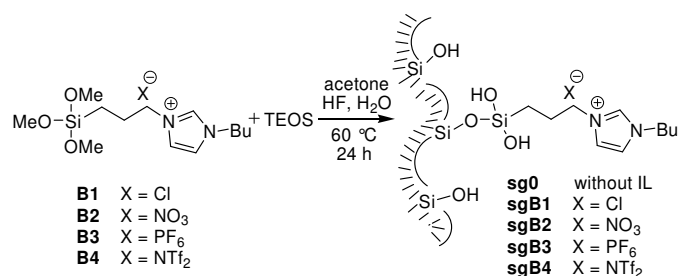
Leandro Luza,<sup>a</sup> Aitor Gual,<sup>a</sup> Camila P. Rambor,<sup>a</sup> Dario Eberhardt,<sup>b</sup> Sérgio R. Teixeira,<sup>b</sup> Fabiano Bernardi,<sup>b</sup> Daniel L. Baptista<sup>b</sup> and Jairton Dupont<sup>a,\*</sup>

**Hybrid organosilicas prepared by sol-gel processes using 1-*n*-butyl-3-(3-trimethoxysilylpropyl)-imidazolium cation associated with hydrophilic and hydrophobic anions can be easily decorated with well dispersed and similar size (1.8-2.1 nm) Pd nanoparticles (Pd-NPs) by simple sputtering-deposition. Higher Pd concentration at the surface compared to the deeper region is obtained in the supports with smaller pore diameter (containing hydrophobic ILs) than those prepared in supports with the largest pore diameter (containing hydrophilic ILs). The IL hydrophobicity plays a central role on the hydrogenation of dienes by controlling the diene access to NP surface active sites.**

The supported ionic liquid phase (SILP) method is emerging as an important alternative for the immobilisation of homotopic transition metal catalysts, in particular for continuous processes.<sup>1,2</sup> More recently, it was demonstrated that the SILP concept could be extended to IL soluble transition metal nanoparticles (M-NPs).<sup>3,4</sup> In these cases, the M-NPs are prepared by classical chemical methods (decomposition of organometallic complexes and/or reduction of metal salts) in the presence of ILs. These M-NPs are used as catalysts for the hydrogenation process since they are usually more active and selective than the classical homotopic and heterotopic catalysts.<sup>5-10</sup> However, from an economic and ecological point of view, the use of “greener” methods of synthesis of M-NPs is more desirable than the classical methods. Thus, the use of ‘green methods’ of M-NPs preparation such as resistive evaporation, laser ablation and magnetron sputtering may be used since they do not change the initial chemical composition, do not use organic solvents and were shown to be fast methods of M-NPs preparation.<sup>11-13</sup> Therefore, the use of sputtering-deposition may constitute one of the simplest and most efficient approaches employed for the generation of new SILP

nanocatalysts. In this respect, our group demonstrated that M-NPs uniformly distributed onto solid supports can be easily prepared by sputtering-deposition (top-down method).<sup>4,14</sup> In particular, the use of a new sputtering chamber with constant mixing of the solid support during the sputtering allowed the generation of small and well-distributed Pd-NPs onto ionic-liquid-modified Al<sub>2</sub>O<sub>3</sub> supports, which displayed comparable catalytic performance in the hydrogenation of 1,3-dienes to those catalysts prepared by conventional chemical methods (bottom-up).<sup>4</sup> It is evident that the use of this new technique for silica could generate more versatile SILP nanocatalysts. In fact, silica is one of most used inorganic supports for the immobilisation of M-NPs; however, in many cases, the use of an extra-stabilising agent anchored to its surface is necessary to improve the catalytic performance of the nanoparticles.<sup>15,16</sup> The use of ILs in the synthesis of hybrid materials, such as organosilicas, has emerged as a new class of supports for M-NPs stabilisation, since a thin film of IL can immobilise and stabilise the nanocatalysts with no mass transfer limitations. Moreover, the structural and textural properties of the hybrid matrix are influenced by the presence of the IL due to its intrinsic organisation and physicochemical properties; its presence could affect the activity and selectivity obtained by the M-NPs.<sup>17-19</sup> Herein, we describe the synthesis and characterisation of surface “clean” Pd-NPs uniformly distributed onto hybrid organosilicas by the sputtering-deposition technique. Most importantly, we show that the imidazolium IL hydrophobicity mainly controlled by the anion nature is the main feature that influences the implantation depth of NPs and the catalytic activity of these SILP nanocatalysts.

The supports **sgB1–sgB4** were prepared using the classical sol-gel process in the presence of IL (**B1–B4**), TEOS, in H<sub>2</sub>O/acetone mixture and an aqueous HF. The support **sg0** was prepared in the absence of IL (Scheme 1).

Scheme 1 Synthesis of the **sg0**–**sgB4** supports.

The **sg0**–**sgB4** hybrid materials have been characterised by <sup>13</sup>C CP-MAS NMR spectra and FT-IR (see Tables S1 and S2 and Figures S1 and S2). N<sub>2</sub> adsorption-desorption isotherms of the **sg0**–**sgB4** supports exhibited pore diameters of 3.1 to 11.6 nm (Table 1) with type-IV isotherm patterns (Figure S3), which are characteristic of mesoporous materials.<sup>20</sup> The surface areas, pore volumes and pore diameter values decreased in the supports containing ILs, and exhibited two distinct patterns: supports with hydrophilic anions (**sgB1** and **sgB2**) showed similar values for textural properties and hysteresis loops, while supports with hydrophobic anions (**sgB3** and **sgB4**) also displayed similar characteristics.

Table 1 Characterisation of the **sg0**–**sgB4** supports.

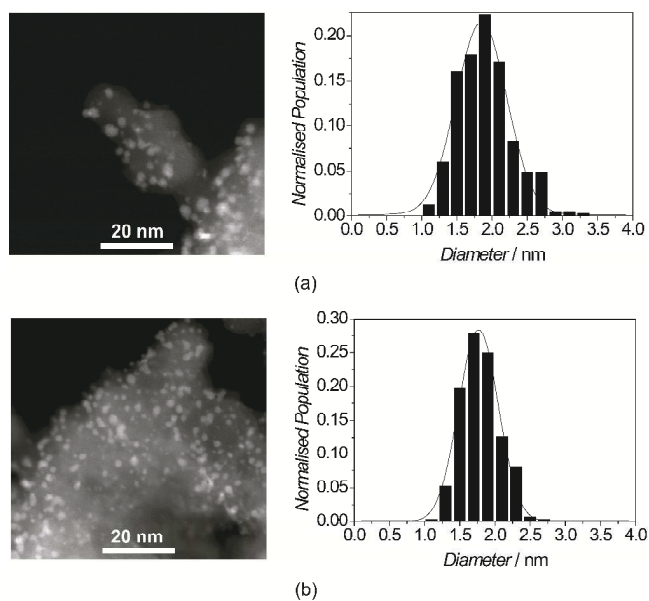
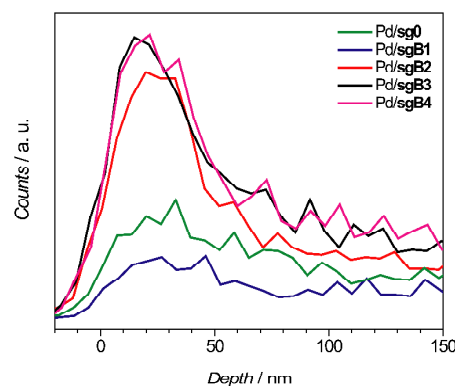
Support	S <sub>BET</sub> /m <sup>2</sup> g <sup>-1</sup>	Pore Volume/cm <sup>3</sup> g <sup>-1</sup> [a]	Pore nm [a]	Diameter/nm	Org. content/mmol IL g <sup>-1</sup> [b]
<b>sg0</b>	469	1.00	11.6	—	—
<b>sgB1</b>	378	0.55	4.5	0.94	
<b>sgB2</b>	454	0.43	3.9	0.51	
<b>sgB3</b>	289	0.14	3.1	0.46	
<b>sgB4</b>	277	0.13	3.2	0.50	

[a] The specific surface areas were determined by the BET multipoint method and the average pore size was obtained by BJH method; [b] Calculated on the basis of the nitrogen content determined by elemental analysis.

The patterns associated with the anions were also observed with the pore diameter distribution, since the supports **sgB3** and **sgB4** displayed narrow distributions and the supports **sgB1** and **sgB2** showed larger distributions. The **sg0** support, which does not contain IL in its structure, exhibited the largest pore diameter distribution among all supports (Figure S4). Therefore, it is clear that the anions of the ILs had an influence on the formation of the organosilicas. Similar behaviour was observed for mesoporous silica synthesised by the sol-gel route using ILs as templates.<sup>21</sup> Elemental analysis revealed that **sgB2**–**sgB4** supports contained lower amounts of IL than the **sgB1** support (Table 1).

For the deposition of Pd-NPs by sputtering technique onto the **sg0**, **sgB1**, **sgB2**, **sgB3** and **sgB4** supports, 35 mA of discharge current was used for 3.0 min. The Pd content on the supported catalysts (Pd/**sg0**, Pd/**sgB1**, Pd/**sgB2**, Pd/**sgB3** and Pd/**sgB4**) was analysed by XRF analysis giving the following Pd concentrations: 0.125 ± 0.02 wt%, 0.124 ± 0.01 wt%, 0.122

± 0.01 wt%, and 0.127 ± 0.02 wt%, 0.123 ± 0.01 wt%, respectively. As expected, the absolute amount of Pd was almost the same for all of the samples, since the same current and time of deposition were used.<sup>12</sup> Interestingly, STEM analysis displayed the formation of small NPs that were uniformly distributed onto the supports with a narrow distribution size (1.8 ± 0.7 nm, 1.8 ± 0.8 nm, 1.8 ± 0.6 nm, 2.1 ± 0.9 nm, and 1.8 ± 0.6 nm, respectively) (Figure 1 and Figure S5). Similar Pd-NPs sizes (1.8–2.1 nm) were obtained for all of the supports indicating that the size of the NPs is controlled by the sputtering-deposition conditions. This fact once again revealed that the sputtering-deposition technique is an interesting alternative for the synthesis of Pd-NPs since appropriate tuning of the sputtering conditions easily controlled their sizes.

Fig. 1 Typical STEM images and histograms of the (a) Pd/**sg0** and (b) Pd/**sgB4** catalysts.Fig. 2 Depth profile of the Pd/**sg0**–Pd/**sgB4** catalysts determined by RBS.

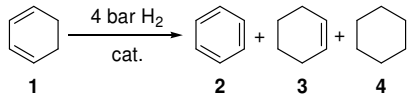
Rutherford backscattering spectrometry (RBS) analysis was used to verify the relative depth profile of imprinted Pd-NPs in the hybrid supports. In fact, the RBS technique can be used to

measure film thicknesses and the depth profile of a known impurity up to a depth of around 1  $\mu\text{m}$  of the sample.<sup>22</sup> The RBS analysis displayed the depth profiles (non-normalised) of the Pd-NPs in the supports (Figure 2). It indicates a dependence of the depth profile shape with the support used.

Comparing Figure 2 and Table 1 it is possible to observe that this dependence is related to the pore diameter of the support. The supports with smaller pore diameter, **sgB3** (3.1 nm) and **sgB4** (3.2 nm), have Pd depth profiles that are narrower with a significantly higher Pd concentration at the surface compared to in deeper regions. On the other hand, the support with the largest pore diameter, **sgB1** (4.5 nm), presents a Pd depth profile with a wider distribution. This indicates that a large pore diameter, which is observed in materials prepared in hydrophilic ILs, facilitates the penetration of Pd-NPs into the support.

In order to evaluate the catalytic performance of these new nanocatalysts, they were applied in the selective hydrogenation of 1,3-cyclohexadiene (**1**) under previously tested conditions (0.1  $\mu\text{mol}$  Pd, 1,3-diene/Pd = 5000,  $\text{CH}_2\text{Cl}_2$ , 4 bar  $\text{H}_2$ , 40°C).<sup>4</sup> The high activities obtained by the catalysts exhibited a behaviour that follows the order:  $\text{TOF}_{\text{Pd/sgB3}} > \text{TOF}_{\text{Pd/sgB4}} > \text{TOF}_{\text{Pd/sg0}} > \text{TOF}_{\text{Pd/sgB2}} > \text{TOF}_{\text{Pd/sgB1}}$ ; i.e., the catalysts containing ILs with hydrophobic anions,  $\text{PF}_6^-$  and  $\text{NTf}_2^-$ , achieved higher activities (3.03 and 2.82  $\text{s}^{-1}$ , respectively) than the catalyst that does not possess IL (1.75  $\text{s}^{-1}$ ) that achieved higher activities than the catalysts containing ILs with hydrophilic anions,  $\text{NO}_3^-$  and  $\text{Cl}^-$  (0.96 and 0.86  $\text{s}^{-1}$ , respectively) (Entries 1-5, Table 2).

**Table 2** Hydrogenation of 1,3-cyclohexadiene by Pd/sg0–Pd/sgB4 catalysts.



Entry <sup>[a,b]</sup>	Catalyst	Conv./ % [t/h]	2/ %	3/ %	4/ %	TOF/ $\text{s}^{-1}$ [c,d]
1	Pd/sg0	98 [1.83]	3	96	1	1.75
2	Pd/sgB1	100 [4.00]	3	96	1	0.86
3	Pd/sgB2	62 [6.00]	3	94	3	0.96
4	Pd/sgB3	100 [2.67]	2	97	1	3.03
5	Pd/sgB4	100 [1.83]	2	98	0	2.82

<sup>[a]</sup> Reaction conditions: 0.1  $\mu\text{mol}$  Pd, 1,3-cyclohexadiene/Pd = 5000, 10 mL of  $\text{CH}_2\text{Cl}_2$ , 4 bar  $\text{H}_2$ , 40°C; <sup>[b]</sup> Conversion and selectivity determined by GC analysis; <sup>[c]</sup> TOF = mol 1,3-cyclohexadiene converted/(mol Pd surface  $\times$  time); <sup>[d]</sup> Calculated from the slope of plots of time vs. TON at low substrate conversions.<sup>23</sup>

Generally, the cyclohexene (**3**) vs. cyclohexane (**4**) rate receives full attention concerning selectivity, and the formation of benzene (**2**), a by-product originating from the hydrogen disproportionation of the diene, is not commonly described in the literature.<sup>24-29</sup> High selectivities for cyclohexene (**3**) (ca. 94-98%) and low amounts of benzene (**2**) (2-3%) were obtained by

the catalysts. Since the Pd-NPs sizes are similar (1.8-2.1 nm) the activities achieved by the catalysts indicate that the IL layer on the surface of the supports had a strong influence in their catalytic performance. This behaviour could be noted by the analysis of the reaction kinetics displayed by the catalysts since only the Pd/sg0 catalyst exhibited an incubation period (Figure S6), which suggest that the solubility and diffusion of the substrate/products/ $\text{H}_2$  until the Pd-NPs can be modified by the IL layer.<sup>30</sup> The Pd/sgB2 catalyst, which contains the  $\text{NO}_3^-$  anion, was deactivated after 6 hours. Indeed, it is known that some Pd catalysts can be poisoned by the formation of cyanide and nitrogen oxides.<sup>31</sup> It is clear that dienes are much more soluble in hydrophobic IL than in hydrophilic ones.<sup>32,33</sup>

Under deuterium, a small kinetic isotopic effect was observed with the Pd/sg0 catalyst ( $\text{H}_2/\text{D}_2$ TOF ratio 1.28) and a greater effect was seen with the Pd/sgB4 catalyst ( $\text{H}_2/\text{D}_2$ TOF ratio 1.96) (Table S3). The kinetic isotopic effect, related to the  $\text{H}/\text{D}^-$  transfer in two steps of the hydrogenation pathways<sup>4</sup> is more pronounced with the Pd/sgB4 catalyst. This is a strong indication that the activation of H-H /D-D bonds is the rate-determining step in this case.<sup>34</sup> Therefore, the IL moiety is acting as a ligand and probably making the Pd surface more electrophilic. A similar ligand/isotopic effect was recently observed on hydrogenation reactions catalysed by cinchonidine-modified Pt/ $\text{Al}_2\text{O}_3$ .<sup>35</sup>

## Conclusions

We have demonstrated that well-dispersed and small-sized Pd nanoparticles can be easily “imprinted” in IL-containing hybrid organosilicas using simple sputtering-deposition. In these cases, the NPs size is not directly controlled by the nature of the IL. However, a higher Pd concentration at the surface compared to deeper regions is obtained in the supports with smaller pore diameters, i.e., those prepared with hydrophobic ILs compared to those prepared in supports with the largest pore diameter (containing hydrophilic ILs). It is also clear that even low amounts of IL have a strong influence on the catalytic performance of SILP Pd nanocatalysts. Thus, the IL hydrophobicity seems to play a central role in controlling the diene access to NP surface active sites and therefore has a strong influence on the catalyst activity (TOF), with a lesser effect on the selectivity. Moreover, the IL thin layer on the Pd NPs surface change the kinetic of the hydrogenation of dienes in view of primary kinetic isotopic effect of  $K_L/K_H = 1.96$  observed in the Pd-NPs implanted in hybrid silica, indicating that the activation of H-H/D-D bonds is the rate-determining step, which is in contrast to that seen with Pd supported on unmodified silica ( $K_L/K_H = 1.28$ ).

## Notes and references

<sup>a</sup> Institute of Chemistry, UFRGS Avenida Bento Gonçalves, 9500 Porto Alegre 91501-970 RS Brazil Fax: (+55) 5133087304 E-mail: jairton.dupont@ufrgs.br

<sup>b</sup> Institute of Physics, UFRGS Avenida Bento Gonçalves, 9500 Porto Alegre 91501-970 RS Brazil

Electronic Supplementary Information (ESI) available: Characterisation for the materials and catalytic reaction data See DOI: 10.1039/c000000x/

1. C. P. Mehnert, E. J. Mozeleski and R. A. Cook, *Chem. Commun.*, 2002, 3010-3011.
2. A. Riisager, P. Wasserscheid, R. v. Hal and R. Fehrmann, *J. Catal.*, 2003, **219**, 452-455.
3. M. A. Gelesky, C. W. Scheeren, L. Foppa, F. A. Pavan, S. L. P. Dias and J. Dupont, *Biomacromol.*, 2009, **10**, 1888-1893.
4. L. Luza, A. Gual, D. Eberhardt, S. R. Teixeira, S. S. X. Chiaro and J. Dupont, *ChemCatChem*, 2013, **5**, 2471-2478.
5. B. Chaudret and K. Philippot, *Oil Gas Sci. Technol.*, 2007, **62**, 799-817.
6. P. Migowski and J. Dupont, *Chem. Eur. J.*, 2007, **13**, 32-39.
7. D. Astruc, *Nanoparticles and Catalysis*, Wiley-VCH, Weinheim 2008.
8. N. Yan, C. X. Xiao and Y. Kou, *Coordin. Chem. Rev.*, 2010, **254**, 1179-1218.
9. C. Vollmer and C. Janiak, *Coordin. Chem. Rev.*, 2011, **255**, 2039-2057.
10. A. Gual, C. Godard, S. Castellón, D. C.-Ferré and C. Claver, *Catal. Today*, 2012, **183**, 154-171.
11. S. Kuwabata, T. Tsuda and T. Torimoto, *J. Phys. Chem. Lett.*, 2010, **1**, 3177-3188.
12. H. Wender, L. F. d. Oliveira, P. Migowski, A. F. Feil, E. Lissner, M. H. G. Prechtel, S. R. Teixeira and J. Dupont, *J. Phys. Chem. C*, 2010, **114**, 11764-11768.
13. H. Wender, R. V. Gonçalves, A. F. Feil, P. Migowski, F. S. Poletto, A. R. Pohlmann, J. Dupont and S. R. Teixeira, *J. Phys. Chem. C*, 2011, **115**, 16362-16367.
14. R. Bussamara, D. Eberhardt, A. F. Feil, P. Migowski, H. Wender, D. P. d. Moraes, G. Machado, R. M. Papaléo, S. R. Teixeira and J. Dupont, *Chem. Commun.*, 2013, **49**, 1273-1275.
15. A. Riisager, B. Jorgensen, P. Wasserscheid and R. Fehrmann, *Chem. Commun.*, 2006, 994-996.
16. C. Meyer, V. Hager, W. Schwieger and P. Wasserscheid, *J. Catal.*, 2014, **292**, 157-165.
17. T. Torimoto, T. Tsuda, K.-i. Okazaki and S. Kuwabata, *Adv. Mater.*, 2010, **22**, 1196-1221.
18. A. Vioux, L. Viau, S. Volland and J. L. Bideau, *C. R. Chim.*, 2010, **13**, 242-255.
19. J. L. Bideau, L. Viau and A. Vioux, *Chem. Soc. Rev.*, 2011, **40**, 907-925.
20. K. S. W. Sing, D. H. Everett, R. A. W. Haul, L. Moscou, R. A. Pierotti, J. Rouquerol and T. Siemieniowska, *Pure & Appl. Chem.*, 1985, **57**, 603-619.
21. J. Zhang, Y. Ma, F. Shi, L. Liu and Y. Deng, *Micro. Meso. Mater.*, 2009, **119**, 97-103.
22. W.-K. Chu, J. W. Mayer and M.-A. Nicolet, *Backscattering Spectrometry*, Academic Press, New York 1978.
23. A. P. Umpierre, E. de Jesus and J. Dupont, *ChemCatChem*, 2011, **3**, 1413-1418.
24. M. Ooe, M. Murata, T. Mizugaki, K. Ebitani and K. Kaneda, *Nano Lett.*, 2002, **2**, 999-1002.
25. J. Huang, T. Jiang, H. Gao, B. Han, Z. Liu, W. Wu, Y. Chang and G. Zhao, *Angew. Chem. Int. Ed.*, 2004, **43**, 1397-1399.
26. P. P. Zweni and H. Alper, *Adv. Synth. Catal.*, 2006, **348**, 725-731.
27. T. Mizugaki, M. Murata, S. Fukubayashi, T. Mitsudome, K. Jitsukawa and K. Kaneda, *Chem. Commun.*, 2008, 241-243.
28. C. Ornelas, J. R. Aranzaes, L. Salmon and D. Astruc, *Chem. Eur. J.*, 2008, **14**, 50-64.
29. R. Tao, S. Miao, Z. Liu, Y. Xie, B. Han, G. An and K. Ding, *Green Chem.*, 2009, **11**, 96-101.
30. A. Riisager, R. Fehrmann, M. Haumann, B. S. K. Gorle and P. Wasserscheid, *Ind. Eng. Chem. Res.*, 2005, **44**, 9853-9859.
31. M. G. Volkonskii, V. A. Likholobov and Y. I. Yermakov, *React. Kinet. Catal. Lett.*, 1982, **21**, 213-218.
32. E. T. Silveira, A. P. Umpierre, L. M. Rossi, G. Machado, J. Morais, G. V. Soares, I. J. R. Baumvol, S. R. Teixeira, P. F. P. Fichtner and J. Dupont, *Chem. Eur. J.*, 2004, **10**, 3734-3740.
33. A. P. Umpierre, G. Machado, G. H. Fecher, J. Morais and J. Dupont, *Adv. Synth. Catal.*, 2005, **347**, 1404-1412.
34. A. Farkas and L. Farkas, *J. Am. Chem. Soc.*, 1938, **60**, 22-28.
35. F. Meemken, A. Baiker, J. Dupré and K. Hungerbühler, *ACS Catal.*, 2014, **4**, 344-354.

## Graphical abstract

Decoration of hybrid silicas with Pd nanoparticles via sputtering-deposition

